New revelations on the nature of organic matter in ice cores

Amanda M. Grannas,[1,2] William C. Hockaday,[1] Patrick G. Hatcher,[1,3] Lonnie G. Thompson,[4] and Ellen Mosley-Thompson[4]

[1] Analysis of organic species stored in ice cores provides a unique opportunity to obtain information about the environment of the past. Because of the trace nature of the organic components of interest, studying these species in molecular level detail within ice cores can be an analytical challenge. Using Fourier transform ion cyclotron resonance mass spectrometry with electrospray ionization, we have characterized, at an unprecedented molecular level, the organic material in an ice core collected from Franz Josef Land (Russia). Several thousand distinct molecular species are identified and provide clues to the principal sources of the organic matter. Humic-like substances have been identified in both modern and ancient ice, despite the remote marine setting of the ice field. Species containing sulfur heteroatoms are far more abundant in the modern ice, indicating that anthropogenic sulfur emissions are also present in the high–molecular weight organic compounds preserved in ice.

1. Introduction

[2] Glaciologists use the chemical information stored in ice to reconstruct the climate and environment of the Earth thousands of years before modern times. A variety of compounds is present in ice cores and can be used as proxies for atmospheric conditions at the time of deposition [*Legrand and Mayewski*, 1997]. However, some species are often present only in trace amounts, and accurate identification and characterization may be analytically challenging. Most paleoclimate studies focus on inorganic species, while studies of organic matter are scant and typically focus only on a small fraction of the total organic matter present. Thus one specific challenge is the characterization of a larger fraction of the organic material present in snow and ice.

[3] A rich record of the input of organic matter is likely preserved in ice cores because of aerosol deposition and snow scavenging of gas phase species during precipitation [*Domine and Shepson*, 2002]. Additionally, it has been shown that organic material in snow and ice is photochemically active, releasing reactive gas phase species to the overlying atmosphere [*Sumner and Shepson*, 1999; *Guimbaud et al.*, 2002; *Grannas et al.*, 2004]. These two observations underline the importance of characterizing the organic material in snow and ice, yet few studies have identified (at the molecular level) the organic material preserved in these media. Most existing analyses have focused on CH_4 [*Raynaud and Chappellaz*, 1993], HCHO [*Staffelbach et al.*, 1991; *Hutterli et al.*, 2002], synthetic pollutants [e.g., *Garbarino et al.*, 2002] and low molecular weight carboxylic acids [*Maupetit and Delmas*, 1994; *Legrand and DeAngelis*, 1996]. *Xie et al.* [2000] identified a number of organic compounds originating from biogenic emission and petroleum residue sources in a Himalayan snowpit. *Grannas et al.* [2004] characterized organic material isolated from snow in the Canadian Arctic and atop the Greenland ice sheet, identifying biogenically derived lipids and lignin. However, both methods required large volumes of snow-derived meltwater (>20 L) in order to isolate sufficient amounts for analysis.

[4] Because of current analytical limitations, it has become commonplace to focus only on "total organic carbon" measurements or specific classes of organic molecules [e.g., *Cachier*, 1995; *Legrand and DeAngelis*, 1996], as no analytical methods exist that can provide a broad-spectrum characterization of the organic material present. Unfortunately, a wealth of information goes uncollected when only a small fraction of the organic material is examined.

[5] A new technique has emerged that is well suited for the characterization of natural organic matter from diverse environments. Electrospray ionization coupled to high-resolution Fourier transform ion cyclotron resonance mass spectrometry (ESI-FTICR-MS) now allows the characterization of complex mixtures of natural organic matter [*Kim et al.*, 2003a; *Kujawinski et al.*, 2002; *Stenson et al.*, 2003]. The technique is useful because electrospray is a "soft" ionization technique causing little fragmentation, thus leaving the parent organic molecules intact. High-resolution detection leads to the ability to resolve peaks varying by 0.0001 m/z (i.e., the molecular weight for singly charged

---

[1]Department of Chemistry, Ohio State University, Columbus, Ohio, USA.
[2]Now at Department of Chemistry, Villanova University, Villanova, Pennsylvania, USA.
[3]Now at Department of Chemistry and Biochemistry, Old Dominion University, Norfolk, Virginia, USA.
[4]Byrd Polar Research Center, Ohio State University, Columbus, Ohio, USA.

ions). Thus it is possible to resolve virtually any (ionizable) organic compound, even in a complex mixture, without a priori chromatographic separation.

2. Experimental Procedure

[6] We employed ESI-FTICR-MS to examine dissolved organic material (DOM) preserved in an ice core obtained from Franz Josef Land, Russia. Cores were collected in 1997 from the Windy Dome Ice Field in Franz Josef Land (80°47′N, 63°32′E, 509 masl). Two cores were drilled (approximately 0.5 m apart), the longest of which was 315 meters and extended back 700 years. After drilling, the cores were packaged in plastic tubing, placed in cardboard tubes, and packed in insulated containers with cryopaks. The containers were shipped to Moscow where they were kept in the airport freezer facility until they were air freighted to Columbus, Ohio. The cores were stored in the Byrd Polar Research Center freezer facility at temperatures of approximately −25°F.

[7] Two core subsections, containing material deposited in approximately 1950 and 1300 A.D. (dated using three seasonally varying parameters; Cl⁻, $\delta^{18}O$ and visible melt layers [*Henderson*, 2002]), were used for ESI-FTICR-MS analysis. These samples were processed as follows: Subsamples were cut from appropriate sections of the core in a cold work room (temp 22°F), placed in precleaned (precombusted glass) containers and transported in a closed case to the Class 100 Clean Room. After rinsing away the outer portion (∼0.5 cm) of the core samples with ultrapure water, they were melted at room temperature in precombusted glass beakers covered with precombusted aluminum foil. Melted samples (900 mLs) were acidified with concentrated hydrochloric acid and passed through a C-18 extraction disk (Empore, 3M), using the approach described by *Kim et al.* [2003b]. The filtrate was passed a second time through the same C-18 extraction disk to ensure efficient extraction of organic material. Ten milliliters of a methanol/water mixture (80%/20% (v/v)) was used to elute the organics from the C-18 disk. The eluent was Teflon capped in a precombusted sample vial and stored at 4°C until analysis. Because of the retention mechanism (hydrophobic adsorption) and small mean pore size of the C-18 resin (60 Angstrom) used in the extraction; we will observe mainly the dissolved fraction of organic material. Organics may also be associated with particulates, but this fraction is currently beyond the scope of this study. Several studies have shown that C-18 recovers 60–100% of the dissolved organics in riverine samples [*Roubeuf et al.*, 2000; *Kim et al.*, 2003b; *Louchouarn et al.*, 2000]. Given the similar functional group distribution of atmospheric HULIS to those of riverine humic substances [*Cappiello et al.*, 2003], it is reasonable to expect that similar quantities of the organics in ice meltwater have been extracted in this study. With regard to selectivity of the disk for certain types of organics, ¹H nuclear magnetic resonance (NMR) experiments show that dissolved organics extracted from river water by C-18 contain a very similar distribution of chemical structures to untreated DOM isolated by evaporation, indicating that C-18 isolates a relatively representative sample. In addition to concentrating the organics from dilute aqueous samples, the C-18 extraction removes inor-

ganic salts and metals that can quench the signal in the NMR spectrometer, and impair ionization within the electrospray source of the mass spectrometer.

[8] The electrospray technique generates ions by spraying the analyte mixture from a syringe across a voltage bias (at atmospheric pressure), where the cathode-anode pair consists of the tip of the syringe and a heated steel capillary, which serves as the spectrometer inlet. As they are forced out of the syringe and through the voltage offset, the surfaces of the droplets are covered with electrostatic charges of the same sign. As the solvents within the droplets evaporate, the charged species are forced closer in proximity to one another until electrostatic repulsions cause the "liftoff" of charged molecules into the gas phase. Organic species that are amenable to this technique are those with redox activity. For example, species that contain one or more acidic or basic functional groups are ionized readily, while analytes such as unsubstituted hydrocarbons and polysaccharides are ionized poorly. The 9.4 Tesla ESI-FTICR-MS housed at the National High Magnetic Field Laboratory (Tallahassee, Florida, USA) was used to analyze the C-18 isolated organic material and blank samples. Samples were analyzed in both positive and negative ion modes; however, positive mode ionized a greater number of organic species. Therefore we only report data obtained in positive ion mode. The sample was injected via syringe pump at a flow rate of 4−5 μL/min. Optimal signal was achieved with a needle voltage of 2500 V and tube lens voltage of 350 V. This particular instrument uses serial octapole mass filters for controlling ion accumulation and transfer into the ion cyclotron resonance cell. Octapole amplitudes, frequencies, and transfer times were optimized for each sample. The time domain signal was averaged for approximately two hours (220 scans) to obtain high-resolution MS spectra. The instrument was calibrated utilizing a dual spray method where a calibrant mix is sprayed alternately with the sample [*Hannis and Muddiman*, 2000]. Resolution of greater than 400,000 was obtained, with mass accuracies typically less than 0.5 ppm error. Blanks (ultrapure water processed in the same manner as the ice core samples) were relatively free of interfering compounds. Samples typically displayed thousands of peaks in the mass spectra, whereas the procedural blank yielded less than 50 peaks. We define a peak as a signal greater than 10x standard deviation of the baseline noise. Additionally, none of the identified peaks in the blank were significant peaks in the sample mass spectra. We should point out, however, that although we can perform a procedural blank for ice core processing, the applicability to the entire process is limited. A true blank would also have to include the analysis of a frozen, clean water sample that had been handled, shipped and stored in the same manner as the original ice core. Because the core was drilled in 1997 and our analysis did not commence until 2003, this type of blank analysis was precluded. However, because we removed the outer portion of the core prior to C-18 extraction and analysis, it is likely that much of the potential contamination would have been removed, as contamination due to coring and storage likely impacts the outer portion of the core.

[9] Despite the improvement in our ability to characterize organic materials from relatively pristine snow and ice samples, there is a drawback in the use of electrospray
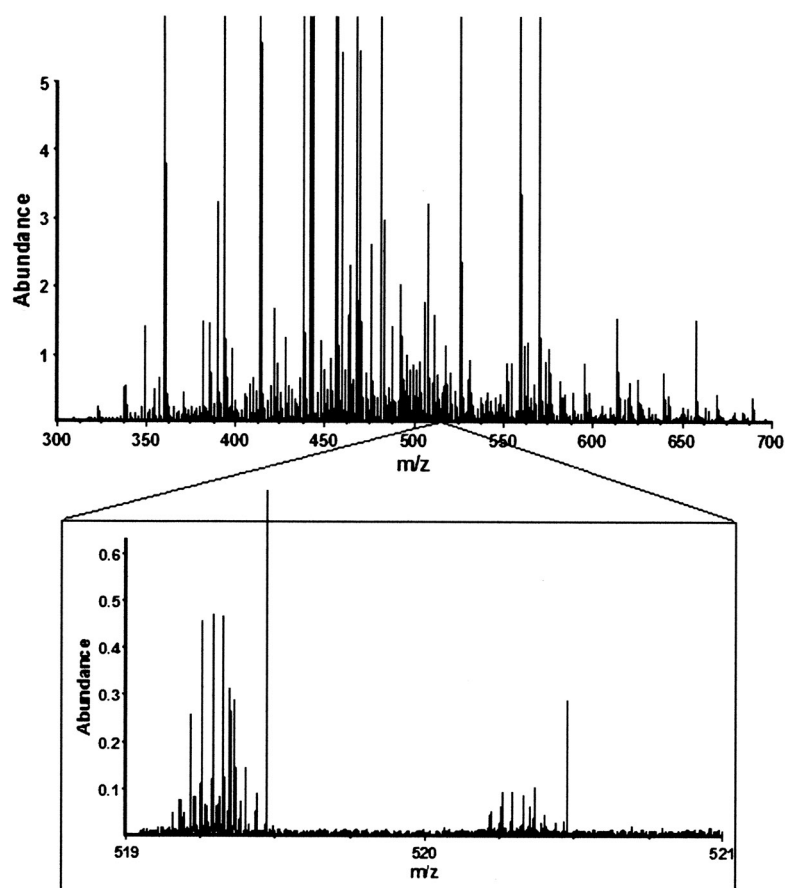
Figure 1. Mass spectrum obtained from ESI-FTICR-MS analysis of a portion of the 1950 A.D. Franz Josef Land ice core (mass unit 519 is expanded to illustrate spectral complexity and identification of ^{13}C analog peaks).

ionization with FTICR detection. The relative abundance detected will not only be related to the amount of the material in the sample, but also to the ease with which the molecule is ionized. Consequently, the method is not yet quantitative. This limitation can be addressed by further studies of the ionization efficiencies of various classes of organic molecules. However, differences among samples that have been prepared and analyzed in the same way can easily be compared using electrospray FTICR analysis, as illustrated here, and provides a new approach for tracking relative changes of organic species within a given ice core (e.g., tracking the seasonality of deposition of a given species or group of organic molecules) or differences in the composition of samples from different locations.

3. Results and Discussion

[10] Following the ESI-FTICR-MS analysis of the C-18 extracted dissolved organic matter, mass spectra were generated with an average resolution of over 400,000 at m/z = 450. It is immediately apparent that the mass spectra are quite complex (Figure 1), as more than 4000 observed peaks were distributed over a range of 300–800 m/z. This corroborates the findings of *Grannas et al.* [2004], where a majority of the total organic carbon present in Arctic snow samples from Canada and Greenland existed as material

less than 1000 Dalton (molecular weight) in size. The complex nature of the organic constituents is further illustrated in the Figure 1 inset, as more than 20 distinct molecular species are typically detected at each nominal mass. The positive ion electrospray process generates positively charged peaks containing an adducted proton or alkali metal cation, usually sodium, ([M+H]$^+$ or [M+Na]$^+$ where M is the neutral molecule). Because most organic compounds have an even mass (depending on their nitrogen content), the majority of peaks will be observed at odd m/z values (i.e., even parent mass plus one proton or one Na). We expect Na to be the most likely metal cation adduct simply because of its prevalence in snowmelt or ice cores and the ease with which it forms an adduct under the electrospray ionization conditions. Most of the peaks at even m/z are the isotope (^{13}C) peaks of molecules showing peaks at odd masses.

[11] Because of the high mass accuracy of the ESI-FTICR-MS method, it is possible to assign distinct empirical formulas to a majority of the peaks present in the mass spectrum using the exact isotopic mass of C, H, N, O, S and Na. Mass spectrometric analysis of the 1300 A.D. sample yielded 4403 discrete peaks (at 10 times the standard deviation of the baseline noise), with positive identification of 3068 elemental formulas (70% of peaks). The 1950 A.D. sample yielded 5329 discrete peaks (at 10 times the standard
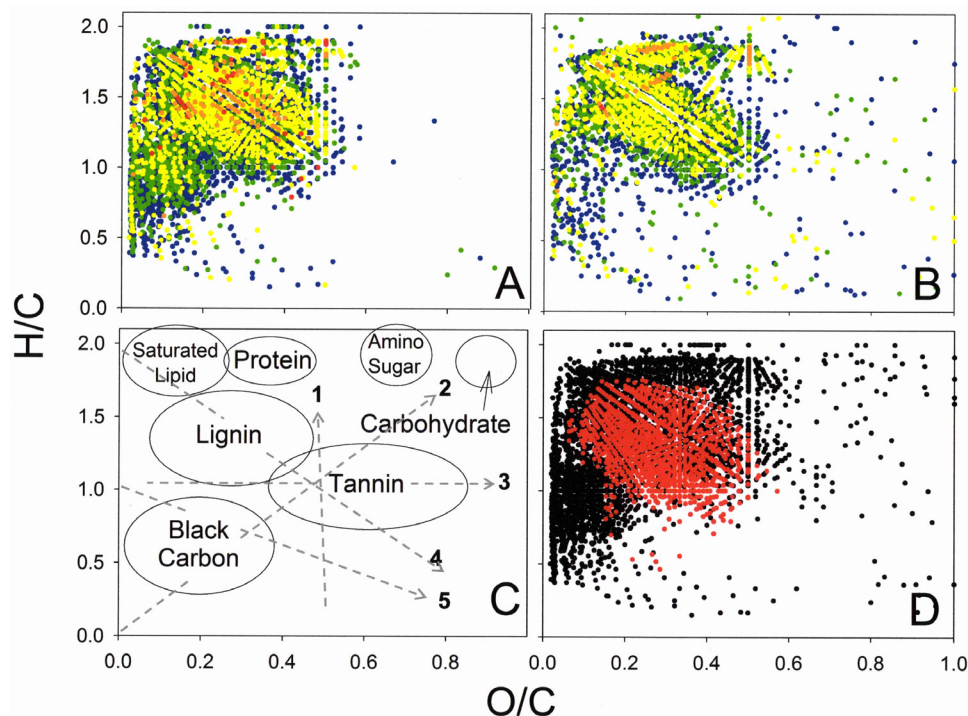
Figure 2. Van Krevelen plots of (a) Franz Josef Land ice core DOM, 1950 A.D. and (b) Franz Josef Land ice core DOM, 1300 A.D. (c) Representative plot illustrating regions where different types of DOM appear. (d) Franz Josef Land ice core DOM, 1950 A.D.; black points are empirical formulas identified in the ice core, and red points are those formulas that exactly match species identified in the Maple River, Michigan, dissolved organic matter sample. Color coding in Figure 2a and 2b represents the mass spectral intensity of the identified peak. Blue represents peaks contributing <0.01% to the total spectrum abundance, green = 0.01–0.05%, yellow = 0.05–0.1%, orange = 0.1–1%, and red = >1%. The lines in Figure 2c illustrate chemical reactions and are noted as (1) hydrogenation or dehydrogenation; (2) hydration or condensation; (3) oxidation or reduction; (4) methylation, demethylation or alkyl chain elongation; and (5) carboxylation or decarboxylation (note that the intercept and slope may differ for pathway 5, depending on the base molecule undergoing reaction).

deviation of the baseline noise), with positive identification of 4430 elemental formulas (83% of the peaks). A process blank yielded few peaks (<50).

[12] *Kim et al.* [2003a] have shown that, once unique elemental formulas are calculated, the large data set consisting of many thousand distinct formulas can be sorted by use of the van Krevelen diagram. When H/C versus O/C (of each distinct empirical formula) is plotted for the two samples examined here, distinct regions corresponding to different types of molecules emerge (Figure 2c). For example, a saturated lipid ($C_xH_{2x}O_2$) will plot in the region near (0,2). As the lipids become more oxidized they will move toward more positive values on the O/C axis, and their trajectories on the van Krevelen diagram will be a line radially extending from the point (0,2). Many such trajectories can be discerned in Figure 2 indicating that there are numerous series of molecules that show homology involving CH$_2$ units. Hydrogen deficient molecules such as condensed hydrocarbons and aromatics derived from black carbon oxidation will be apparent at low H/C values [*Kim et al.*, 2003a, 2004]. Figures 2a and 2b show the van Krevelen diagrams from compounds detected in the FTICR-MS data of the Franz Josef Land core samples of 1950 A.D. and 1300 A.D., respectively. Colors indicate mass spectral

abundance. It is apparent from the atom ratios that most compounds in the Franz Josef Land core section are relatively saturated (e.g., lipid-like materials and lignin-like materials). Some species are present within the region expected for black carbon as defined by *Kim et al.* [2004], but these make up a relatively small proportion of the peaks. Black carbon-like species account for approximately 2% of the total mass spectral abundance in each sample.

[13] Displaying the information obtained from the mass spectrum in the form of a van Krevelen diagram is useful for several reasons. Thousands of peaks are observed in the FTICR mass spectrum, each with a distinct elemental formula. Utilizing the van Krevelen diagram enables one to characterize the organic matter in a "snapshot" and determine what types of molecules likely compose the sample. For example, from Figure 2a one can assess the relatively low degree of oxidation of the organic materials (most points have O/C ratios less than 0.5) and the relatively saturated nature of the organic materials (most points have H/C ratios >1.0). Additionally, linear trends between data on the van Krevelen plot are suggestive of structural relationships among families of compounds as illustrated in Figure 2c [*Kim et al.*, 2003a]. For example, data points trending along vertical lines represent hydrogenation or
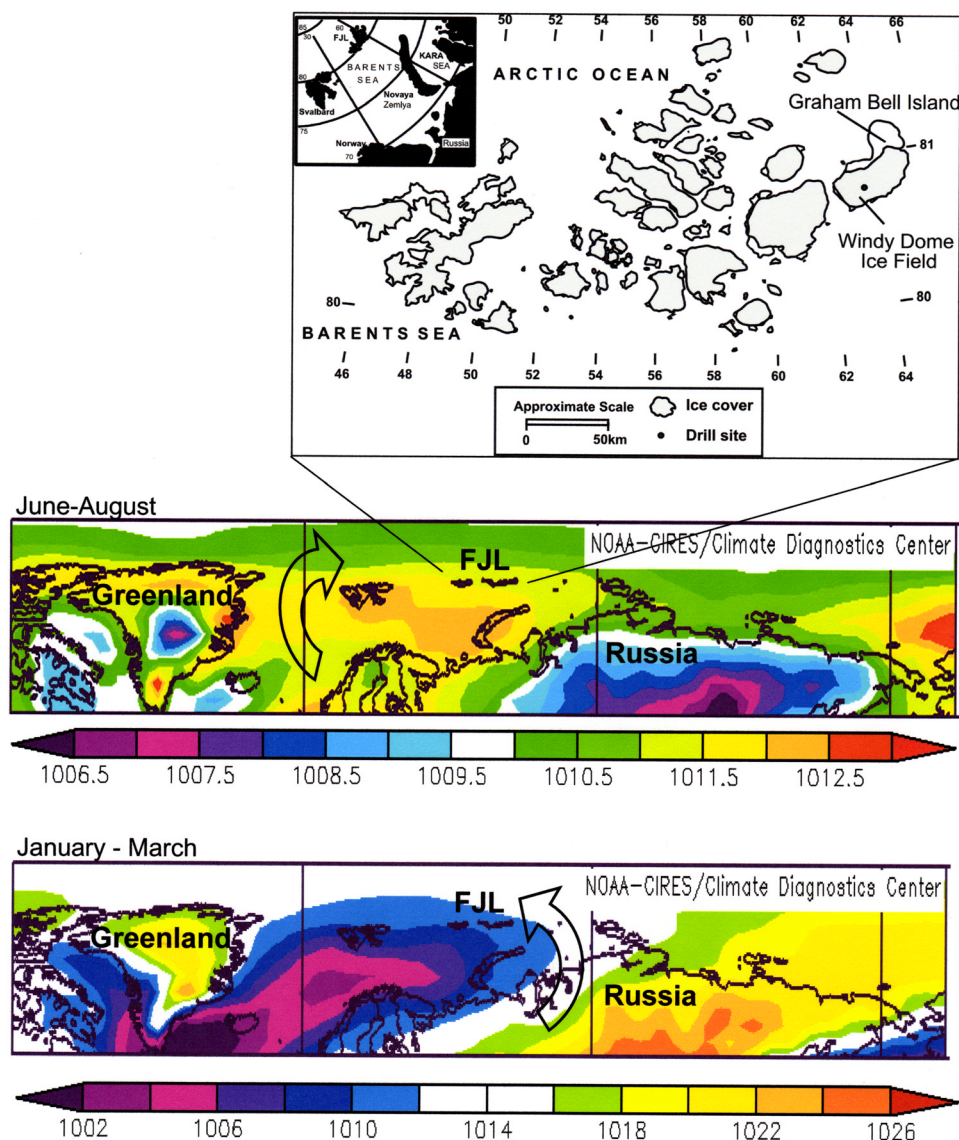
Figure 3. Map of atmospheric circulation patterns for the Franz Josef Land region. Image provided by the NOAA-CIRES Climate Diagnostics Center, Boulder, Colorado, from their website at http://www.cdc.noaa.gov. Inset is a detailed map of Franz Josef Land, showing location of Windy Dome Ice Field.

dehydrogenation differences among molecules; a line with slope of −2 and y axis intercept of 2 represents the loss of CH_2 groups from a saturated compound with gain of oxygen and one unit of unsaturation (e.g., loss of 2 hydrogen atoms); a line with a slope of +2 represents hydration or dehydration. A number of these linear trends are evident in the data from the Franz Josef Land ice core.

[14] Potential sources of the organic material recovered from this particular ice sample could include local material as well as that transported atmospherically from more distant sources. Incorporation of organic material into snow and ice in polar regions has been previously identified [*Calace et al.*, 2001] and likely results from either sea surface aerosol formation that incorporates surface layer organics or from long-range transport from terrestrial sources. *Grannas et al.* [2004] identified lignin in the snow deposited at Summit, Greenland. This site is situated atop the

Greenland ice sheet at 3200 m altitude and is far removed from any vegetation sources. Thus the only plausible mechanism for lignin incorporation into the snowpack is via long-range atmospheric transport. Long-range transport of organic matter would also be expected at the Franz Josef Land ice core site. Interestingly, a comparison of the molecular species identified in the 1950 ice with those isolated from a river in northern Michigan (Maple River) showed striking similarities [*Hockaday et al.*, 2006]. Figure 2d shows the data points for the peaks identified in the 1950 A.D. sample (in black and red). Red points, however, indicate data that exactly match empirical formulas for organic compounds found in FTICR-MS data from a Maple River, Michigan dissolved organic matter sample. It is important to note that the general region where exact matches are observed overlaps with the region where terrestrially derived species such as lignin and tannins plot

on the van Krevelen diagram (Figure 2c), indicating that terrestrial plant biopolymers may be important constituents of the organic matter stored within the ice of this remote marine region.

[15] Atmospheric circulation conditions for Arctic regions have been studied extensively [Barrie, 1986]. Figure 3 illustrates the typical air mass trajectories for winter and spring for this geographical location. In winter and spring, air masses on an eastward trajectory over the Eurasian landmass will encounter a semipermanent Siberian high-pressure regime and will be deflected toward the Kara and Barents seas and then toward the Polar Basin [Simoes and Zagorodnov, 2001; Barrie, 1986]. Along this trajectory, Franz Josef Land (79–80°N and 42–65°E) and Svalbard (74–80°N and 10–35°E) are the first landmasses immediately in the path of air masses that are likely to have been influenced by anthropogenic emissions and terrestrially derived material. In summer, deposited species originate mainly from northeastern North America (although they arrive after significant precipitation has already occurred over the ocean) [Simoes and Zagorodnov, 2001]. Several studies have shown that the Svalbard atmosphere is significantly affected by species derived from midlatitudes, including sulfates [Rahn, 1981], pesticides [Oehme and Ottar, 1984] and organic gases [Hov et al., 1984]. Nickus [2003] reported that much of the snowpack ion content of Franz Josef Land could be explained by sea salt aerosol. There was also evidence of soil-derived dust, however this accounted for only a random variability of the snow chemistry (of ions) at Franz Josef Land. Nickus [2003] also discusses that varying exposure to potentially pollutant-laden air masses was illustrated by the higher concentrations of non-sea-salt sulfate found in snow at Franz Josef Land ($5-10$ μeq L^{-1}) as compared to, for example, Greenland snow (<2 μeq L^{-1}) or interior Alaskan snow (up to 6 μeq L^{-1}). Total sulfate concentrations measured in our samples ranged from 3.5 to 23 μeq L^{-1}, with much less sulfate measured in the 1300 A.D. sample as compared to the 1950 A.D. sample (average of 3.5 μeq L^{-1} and 15.2 μeq L^{-1}, respectively). Other anthropogenic indicators, including ammonium and nitrate, are both elevated in the 1950 A.D. sample relative to the 1300 A.D. sample. Ammonium concentrations (1300 A.D. versus 1950 A.D.) were 1.10 μeq L^{-1} and 2.55 μeq L^{-1}, respectively. Nitrate concentrations (1300 A.D. versus 1950 A.D.) were 0.82 μeq L^{-1} and 2.34 μeq L^{-1}, respectively.

[16] The FTICR-ESI-MS analysis of the Franz Josef Land ice core samples points to the prevalence of organic species whose empirical formulas are common to those previously identified in terrestrial samples [Hockaday et al., 2006]. This is an intriguing finding, and substantiates previous work that identified lignin and biogenic fatty acids in snow deposited atop the Greenland glacier and in the high Canadian Arctic [Grannas et al., 2004]. These findings also corroborate recent studies that highlight the potential importance of humic-like substances present in atmospheric waters [Cappiello et al., 2003; Yang et al., 2004]. Additionally, this technique provides significant improvements to the data currently available in the scientific literature, as we can now identify these components by their unique empirical formulas, rather than generalized, bulk characteristics.
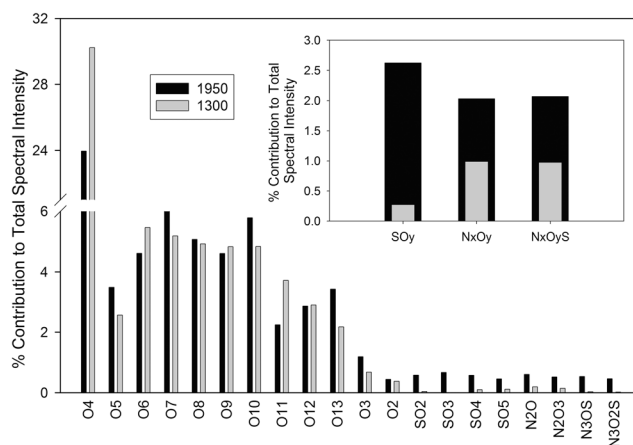

Figure 4. Comparison of the elemental formulas identified in the 1950 A.D. sample and 1300 A.D. sample and (inset) the heteroatoms present in both samples. The x axis represents the "functionality" present in the formula C_xH_yZ, where Z is the atoms shown at each bar on the x axis.

[17] From the FTICR-MS data, it is also possible to compare the "functionality" distribution apparent in the organic material identified in various samples. Figure 4 shows the most abundant species identified in each core sample. This was determined by sorting all of the identified peaks by their empirical formula and grouping formulas on the basis of heteroatom content (oxygen, nitrogen and sulfur) regardless of the carbon and hydrogen distribution. The measured relative peak abundances of each "subgroup" were then summed and compared to the total peak abundance of all peaks in the spectrum. The percent contribution of each "subgroup" is plotted as the y axis. For example, formulas containing any number of carbon and hydrogen atoms and exactly four oxygen atoms were considered one "functionality" and plotted in Figure 3 as the C_xH_y"O_4" group. Data of this nature allow for comparisons of the organic material present in both samples, and will be a powerful tool for the detection of differences in the distribution of organic species throughout a core profile. As shown in Figure 4, empirical formulas containing $C_xH_yO_4$ are by far the most abundant ions generated by electrospray in both ice cores. Lower oxygenated species ($C_xH_yO_2$ and $C_xH_yO_3$) were identified although are much less abundant. C_xH_y and $C_xH_yO_1$ make up only a small fraction of the identified compounds. Carbon numbers range from 19 to 44. Therefore these species cover a range of molecular weights and could be unsaturated dicarboxylic acids, although further structural elucidation would require application of tandem MS/MS techniques.

[18] Additionally, we have calculated the spectral intensity of the most abundant compounds containing nitrogen and sulfur heteroatoms. It is apparent from Figure 4 (inset) that sulfur-containing species contribute more strongly to the DOM in the 1950 A.D. ice core section as compared to the 1300 A.D. core section. In fact, in the 1950 A.D. sample, 21% of all identified empirical formulas contained sulfur (the rest had no sulfur). In the 1300 A.D. sample,
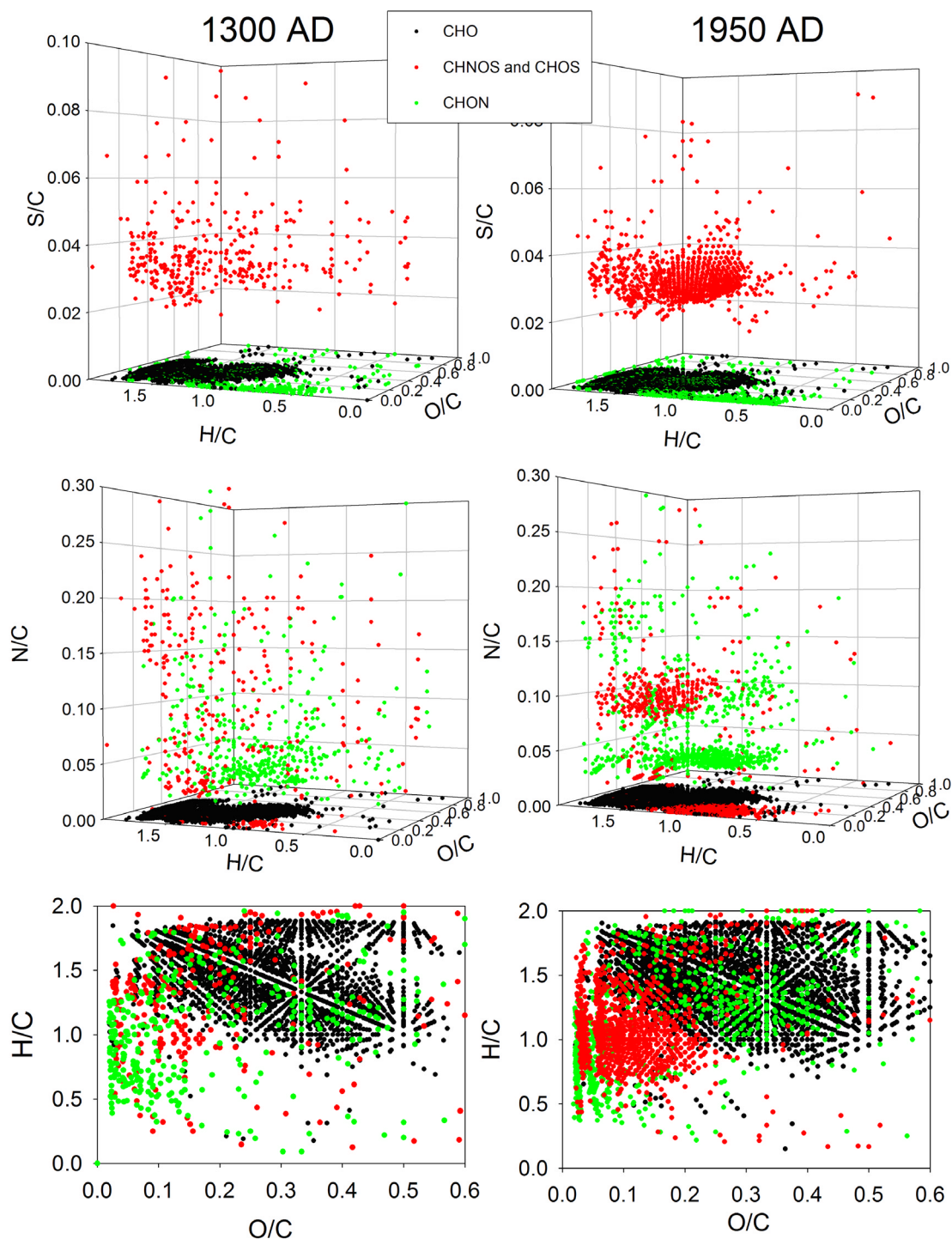
Figure 5. Van Krevelen plots of the molecular formulas identified in Franz Josef Land ice deposited circa (left) 1300 A.D. and (right) 1950 A.D. (top) Three-dimensional plots illustrating the sulfur content (S/C ratio shown as z axis). (middle) Three-dimensional plots illustrating the nitrogen content (N/C ratio shown as z axis). (bottom) Two-dimensional plot illustrating H/C and O/C ratios identified. Red points indicate molecular formulas containing CHNOS and CHOS atoms. Green points indicate molecular formulas containing CHNO atoms. Black points illustrate molecular formulas containing CHO atoms.

only 12% of identified elemental formulas contained sulfur (the rest had no sulfur). Figure 5 illustrates the distinct regions where many of the sulfur- and nitrogen-containing species plot on the van Krevelen diagram, and highlights the

striking difference between the materials identified in the two cores with respect to sulfur content. Expansion of the two dimensional van Krevelen diagram to a third dimension (using S/C or N/C atom ratio) facilitates visualization of the

Table 1. Most Abundant Molecular Formulas Identified in Both Ice Core Samples[a]

	1950 Core Sample					1300 Core Sample		
Formula	Error in Formula Mass, ppm	Peak Abundance	Formula	Error in Formula Mass, ppm	Peak Abundance	Formula	Error in Formula Mass, ppm	Peak Abundance
$C_{28}H_{40}O_4$	0.3	100	$C_{25}H_{20}SO$	−0.1	0.06	$C_{28}H_{40}O_4$	0.2	100
$C_{29}H_{42}O_4$	0.0	47.9	$C_{25}H_{22}SO$	−0.2	0.04	$C_{29}H_{42}O_4$	−0.2	52.4
$C_{26}H_{36}O_4$	0.2	45.4	$C_{25}H_{24}SO$	0.1	0.06	$C_{26}H_{36}O_4$	0.2	35.7
$C_{24}H_{18}O_{10}$	0.4	26.5	$C_{25}H_{26}SO$	0.0	0.04	$C_{19}H_{34}O_6$	−0.3	14.3
$C_{24}H_{44}O_{12}$	0.2	24.2	$C_{25}H_{20}SO_2$	−0.5	0.17	$C_{26}H_{48}O_{13}$	0.2	13.7
$C_{26}H_{48}O_{13}$	0.3	21	$C_{25}H_{22}SO_2$	0.6	0.11	$C_{24}H_{44}O_{12}$	0.2	12.7
$C_{27}H_{26}O_{13}$	0.4	10.4	$C_{25}H_{24}SO_2$	0.4	0.07	$C_{22}H_{40}O_{11}$	0.1	10.7
$C_{30}H_{44}O_4$	0.4	8.3	$C_{25}H_{20}SO_3$	0.2	0.09	$C_{29}H_{46}O_7$	0.1	9.9
$C_{24}H_{40}O_4$	0.1	7.8	$C_{25}H_{22}SO_3$	−0.6	0.06	$C_{30}H_{44}O_4$	0.1	8.7
$C_{29}H_{46}O_7$	0.2	5	$C_{25}H_{24}SO_3$	0.5	0.06	$C_{20}H_{36}O_{10}$	0.2	7.7
$C_{26}H_{42}N_4O_4$	0.2	4	$C_{26}H_{24}SO_3$	0.5	0.10	$C_{27}H_{42}O_6$	−0.2	6.9
$C_{29}H_{50}O_4$	0.0	3.6	$C_{26}H_{26}SO_3$	0.8	0.06	$C_{35}H_{58}O_{10}$	0.6	6.0
$C_{25}H_{30}O_{11}$	0.1	3.2	$C_{27}H_{22}SO_3$	0.0	0.13	$C_{24}H_{40}O_4$	−0.1	5.9

[a]A sulfur series identified in the modern core is also shown for illustrative purposes. The error in formula mass is calculated by comparing the exact mass of the proposed molecular formula to the mass measured by FTICR-MS. In all cases, the mass error is less than 1 ppm (part per million).

heteroatom distribution. Striking differences arise when utilizing plots in this manner.

[19] Although we observe a significant amount of organosulfur species in the 1950 core section, the origin of these species is currently unknown. Most anthropogenic sulfur emissions from fossil fuel combustion are in the form of sulfur dioxide (SO_2), and the remainder is mainly sulfate species [Lelieveld et al., 1997]. In addition to their influence upon the radiative balance of the atmosphere [Charlson et al., 1992] and acid precipitation [Whelpdale et al., 1997], the role of these sulfur species in aerosol formation is an issue of intense study [e.g., Thornton et al., 1997; Notholt et al., 2005]. Likewise, organic species, both biogenic and anthropogenic, are being studied for their collective role in particle formation and reactivity as pertains to the atmosphere's oxidizing capacity and climate forcing [Kanakidou et al., 2005]. Upon review of the literature on atmospheric organosulfur compounds, research efforts to date have focused primarily on biogenic species of low molecular weight such as dimethylsulfide, dimethylsulfoxide, mercaptans, carbon disulfide, and various other disulfides with short alkene sidechains. However, there is no precedent in the atmospheric literature (to our knowledge) regarding the provenance of the large (C_{17}–C_{45}) organic sulfur species that have been identified in this study. The greater abundance and diversity of these species in the modern ice implicates an anthropogenic source, and we feel that a speculative synthesis is warranted. By analogy to other pollutants, these compounds could be present because of primary emission or secondary products whose formation has been enhanced by various anthropogenic forcings, the most obvious of which include (1) direct emission from a fossil fuel related source, (2) the reaction of anthropogenic SO_2 with atmospheric HULIS, and (3) the formation of reactive organosulfur intermediates from the reaction of biogenic organosulfur compounds with anthropogenic oxidants (e.g., ozone, hydroxyl radical). Diagenetic formation within the ice cannot be discounted, though reaction kinetics in the solid phase are much less favorable. With regard to the first case (direct emission), we found no evidence in the literature for large organics such as those observed in our study. There are numerous examples of oxidation

reactions affecting organosulfur compounds such as dimethyl sulfide (case 3) [e.g., Barnes et al., 1996; Atkinson et al., 1997]. However, the formation of high–molecular weight compounds in the aerosol phase has not been discussed. Nevertheless, case 2 seems worthy of further discussion, considering the high reactivity of SO_2 gas with oxidized organics. For example, the preservative action of SO_2 used in the commercial beverage industry is thought to be due to the spontaneous covalent adduct formation with carbonyl and amino functional groups. This highly exothermic reaction results in a stable bisulfite (SO_3H) adduct to the Schiff base formed by intermolecular interaction of carbonyl compounds with amino compounds [Ingles, 1967]. Sulfur dioxide is also known to cause copolymerization of a number of open chain and cyclic monoalkenes, dienes, and acetylenes at room temperature [Hazell and Ivin, 1962; Ivin and Walker, 1971]. Perhaps the most notable example for its atmospheric relevance are the sulfonated terpolymers of isoprene and piperylene: $[SO_2CH_2CH = CHCH(CH_3)]$ and $[SO_2CH_2CH = C(CH_3)CH_2]$ [Ivin and Walker, 1971]. More recently, sulfuric acid catalyzed aldol condensation of aldehydes and ketones has been recognized for the ability to form UV light-absorbing dienes in atmospheric aerosols [Noziere and Esteve, 2005]. These compounds would serve as suitable precursors to the previously mentioned reaction. Though the relevance of these reactions to the atmosphere has not been demonstrated directly, they do provide an atmospheric context for the interpretation of the organosulfur compounds observed within the modern ice that we characterized.

[20] The molecular formulas corresponding to the most abundant peaks in both cores are shown in Table 1. Several families are apparent, varying either by CH_2 chain length or degree of saturation. An unsaturated CH_2 series is observed ($C_{26}H_{36}O_4$, $C_{28}H_{40}O_4$, $C_{29}H_{42}O_4$, $C_{30}H_{44}O_4$), as well as species that are more highly oxygenated. Dicarboxylic acids are a ubiquitous component of atmospheric organic material [Chebbi and Carlier, 1996]; however, previous studies have typically focused on the characterization and quantification of lower–molecular weight species [e.g., Kawamura and Kaplan, 1985]. Our results indicate that relatively high molecular weight dicarboxylic acids (up to C_{44}) may also

be present in atmospheric aerosols in appreciable amounts. More highly oxygenated species generally plot in the region indicative of lignin (Figure 2c) and could represent the polycarboxylic acids previously proposed as "humic-like substances" (HULIS) in atmospheric water-soluble organics [*Cappiello et al.*, 2003; *Gelencser et al.*, 2002]. The evidence for the abundance of terrestrially derived HULIS in these samples is particularly convincing, as a number of the formulas identified in the ice core samples were also found in terrestrial riverine dissolved organic matter (Figure 2d).

[21] Additionally, a sulfur family (from the 1950 A.D. sample) is shown as an example of the type of heteroatom containing peaks that are present in the modern core. For species of the general formula $C_xH_yO_zS$, carbon numbers ranged from 17 to 45, and oxygen from 1 to 16. The average H/C ratio was 0.99 and the average O/C ratio was 0.13. It is important to note that the list shown in Table 1 is by no means comprehensive, as several thousand distinct formulas were identified in both samples. A comprehensive list of all species identified in the ancient and modern core samples is available from the corresponding authors upon request.

4. Conclusions

[22] We have applied a unique method, electrospray ionization high-resolution Fourier transform ion cyclotron resonance mass spectrometry, to characterize the dissolved organic matter in both modern and ancient ice from Franz Josef Land, Russia. Several thousand compositionally unique molecular species were identified, providing an unprecedented look at the nature of the organic matter preserved in this remote ice field. We employed several graphical methods, including two-dimensional and three-dimensional van Krevelen diagrams and functionality distribution plots, to facilitate the display of a complicated data set and illustrate differences arising between the samples. Humic-like substances with empirical formulas similar to those from terrestrial sources constitute a significant portion of the organic material isolated, despite the ice core's remote marine location. Sulfur containing organics were identified primarily in the postindustrial ice sample, pointing to a potential modern combustion-derived source. The source of these organosulfur compounds is not known, but production due to secondary processes (sulfur oxide reaction with atmospheric organic material) is the leading hypothesis on the basis of evidence currently available in the scientific literature.

[23] As analytical capabilities improve, it is likely that future efforts will be directed toward understanding not only the elemental composition, but also the structural composition of these diverse and complicated organic materials (i.e., via MS/MS techniques that allow for further characterization of molecular fragmentation patterns). Studies of ionization efficiency and matrix effects are required so that the FTICR-MS method moves from qualitative to quantitative. However, the use of Fourier transform ion cyclotron resonance mass spectrometry will likely prove a unique and useful tool for the glaciology community. The technique shows great promise for improving our understanding of the molecules preserved in ice and therefore of changes in biospheric and atmospheric compositions of the past.

References

Atkinson, R., D. L. Baulch, R. A. Cox, R. F. Hampson Jr., J. A. Kerr, M. J. Rossi, and J. Troe (1997), Evaluated kinetic data and photochemical data for atmospheric chemistry: Supplement IV-IUPAC committee on gas kinetic data evaluation for atmospheric chemistry, *J. Phys. Chem. Ref. Data*, *26*, 1392–1499.

Barnes, I., K. H. Becker, and I. Patroescu (1996), FTIR product study of OH initiated oxidation of dimethylsulfide: Observation of carbonyl sulfide and dimethylsulfoxide, *Atmos. Environ.*, *30*, 1805–1814.

Barrie, L. A. (1986), Arctic air pollution: An overview of current knowledge, *Atmos. Environ.*, *20*, 643–663.

Cachier, H. (1995), Combustion of carbonaceous aerosols in the atmosphere: Implications for ice core studies, in *Ice Core Studies of Global Biogeochemical Cycles*, *NATO ASI Ser, Ser. I*, vol. 30, edited by R. Delmas, pp. 313–346, Springer, New York.

Calace, N., B. M. Petronio, R. Cini, A. M. Stortini, B. Pampaloni, and R. Udisti (2001), Humic marine matter and insoluble materials in Antarctic snow, *Int. J. Environ. Anal. Chem.*, *79*, 331–348.

Cappiello, A., E. De Simoni, C. Fiorucci, F. Mangani, P. Palma, H. Trufello, S. Decasari, M. C. Facchini, and S. Fuzzi (2003), Molecular characterization of the water-soluble organic compounds in fogwater by ESIMS/ MS, *Environ. Sci. Technol.*, *37*, 1229–1240.

Charlson, R. J., S. E. Schwartz, J. M. Hales, R. D. Cess, J. A. Coakley Jr., J. E. Hansen, and D. J. Hofmann (1992), Climate forcing by anthropogenic aerosols, *Science*, *255*, 423–430.

Chebbi, A., and P. Carlier (1996), Carboxylic acids in the troposphere, occurrence, sources and sinks: A review, *Atmos. Environ.*, *30*, 4233–4249.

Domine, F., and P. B. Shepson (2002), Air-snow interactions and atmospheric chemistry, *Science*, *297*, 1506–1510.

Garbarino, J. R., E. Snyder-Conn, T. J. Leiker, and G. L. Hoffman (2002), Contaminants in Arctic snow collected over northwest Alaskan sea ice, *Water Air Soil Pollut.*, *139*, 183–214.

Gelencser, A., A. Hoffer, Z. Krivacsy, G. Kiss, A. Molnar, and E. Meszaros (2002), On the possible origin of humic matter in fine continental aerosol, *J. Geophys. Res.*, *107*(D12), 4137, doi:10.1029/2001JD001299.

Grannas, A. M., P. B. Shepson, and T. R. Filley (2004), Photochemistry and nature of organic matter in Arctic and Antarctic snow, *Global Biogeochem. Cycles*, *18*, GB1006, doi:10.1029/2003GB002133.

Guimbaud, C., et al. (2002), Snowpack processing of acetaldehyde and acetone in the Arctic atmospheric boundary layer, *Atmos. Environ.*, *36*, 2743–2752.

Hannis, J. C., and D. C. Muddiman (2000), A dual electrospray ionization source combined with hexapole accumulation to achieve high mass accuracy of biopolymers in Fourier transform ion cyclotron resonance mass spectrometry, *J. Am. Soc. Mass Spectrom.*, *11*, 876–883.

Hazell, J. E., and K. J. Ivin (1962), Relative reactivities of olefins in polysulfone formation, *Trans. Faraday Soc.*, *58*, 176–185.

Henderson, K. A. (2002), An ice core paleoclimate study of Windy Dome, Franz Josef Land (Russia): Development of a recent climate history for the Barents Sea, Ph.D. dissertation, Ohio State Univ., Columbus.

Hockaday, W. C., A. M. Grannas, S. Kim, and P. G. Hatcher (2006), Direct molecular evidence for the degradation and mobility of black carbon in soils from ultrahigh-resolution mass spectral analysis of dissolved organic matter from a fire-impacted forest soil, *Org. Geochem.*, in press.

Hov, O., S. A. Penkett, I. S. A. Isaksen, and A. Semb (1984), Organic gases in the Norwegian Arctic, *Geophys. Res. Lett.*, *11*, 425–428.

Hutterli, M. A., R. C. Bales, J. R. McConnell, and R. W. Stewart (2002), HCHO in Antarctic snow: Preservation in ice cores and air-snow exchange, *Geophys. Res. Lett.*, *29*(8), 1235, doi:10.1029/2001GL014256.

Ingles, D. L. (1967), Some novel adducts of sulphur dioxide with carbonyls and amino acids, *Chem. Ind.*, *35*, 1402–1493.

Ivin, K. J., and N. A. Walker (1971), Relative reactivities of some dienes and acetylenes in copolymerization with sulfur dioxide, *J. Polymer Sci., Part A-1*, *9*, 2371–2375.

Kanakidou, M., et al. (2005), Organic aerosol and global climate modeling: A review, *Atmos. Chem. Phys.*, 5, 1053–1123.

Kawamura, K., and I. R. Kaplan (1985), Determination of organic acids (C_1–C_{10}) in the atmosphere, motor exhausts, and engine oils, *Environ. Sci. Technol.*, 19, 1082–1086.

Kim, S., R. W. Kramer, and P. G. Hatcher (2003a), Graphical method for analysis of ultrahigh-resolution broadband mass spectra of natural organic matter, the Van Krevelen diagram, *Anal. Chem.*, 75, 5336–5344.

Kim, S., A. J. Simpson, E. B. Kujawinski, M. A. Freitas, and P. G. Hatcher (2003b), Non-invasive advanced spectroscopic methods (electrospray ionization mass spectrometry and 2D solution NMR) for analysis of DOM isolated by C_{18} solid phase disk extraction, *Org. Geochem.*, 34, 1325–1335.

Kim, S., L. A. Kaplan, R. Benner, and P. G. Hatcher (2004), Hydrogen-deficient molecules in natural riverine water samples-evidence for the existence of black carbon in DOM, *Mar. Chem.*, 92, 225–234.

Kujawinski, E. B., M. A. Freitas, X. Zang, P. G. Hatcher, K. B. Green-Church, and B. R. Jones (2002), The application of electrospray ionization mass spectrometry (ESI MS) to the structural characterization of natural organic matter, *Org. Geochem.*, 33, 171–180.

Legrand, M., and M. DeAngelis (1996), Light carboxylic acids in Greenland ice: A record of past forest fires and vegetation emissions from the boreal zone, *J. Geophys. Res.*, 101, 4129–4145.

Legrand, M., and P. Mayewski (1997), Glaciochemistry of polar ice cores: A review, *Rev. Geophys.*, 35, 219–243.

Lelieveld, J., G. J. Roelofs, L. Ganzeveld, J. Feichter, H. Rodhe, J. Plane, D. J. Fish, G. P. Ayres, M. H. Smith, and R. A. Cox (1997), Terrestrial sources and distribution of atmospheric sulphur, *Philos. Trans. R. Soc. London, Ser. B*, 352, 149–158.

Louchouarn, P., S. Opsahl, and R. Benner (2000), Isolation and quantitation of dissolved lignin from natural waters using solid phase extraction and GC/MS, *Anal. Chem.*, 72, 2780–2787.

Maupetit, F., and R. J. Delmas (1994), Carboxylic acids in high-elevation Alpine glacier snow, *J. Geophys. Res.*, 99, 16,491–16,500.

Nickus, U. (2003), Ion content of the snowpack on Franz Josef Land, Russia, *Arct. Antarct. Alpine Res.*, 35, 399–408.

Notholt, J., et al. (2005), Influence of tropospheric SO_2 emissions on particle formation and the stratospheric humidity, *Geophys. Res. Lett.*, 32, L07810, doi:10.1029/2004GL022159.

Noziere, B., and W. Esteve (2005), Organic reactions increasing the absorption index of atmospheric sulfuric acid aerosols, *Geophys. Res. Lett.*, 32, L03812, doi:10.1029/2004GL021942.

Oehme, M., and B. Ottar (1984), The long-range transport of polychlorinated hydrocarbons to the Arctic, *Geophys. Res. Lett.*, 11, 1134–1136.

Rahn, K. A. (1981), Arctic air chemistry, *Atmos. Environ.*, 15, 1345–1516.

Raynaud, D., and J. Chappellaz (1993), The record of atmospheric methane, in *Global Environmental Change*, *NATO ASI Ser., Ser. I*, vol. 13, pp. 38–61, Springer, New York.

Roubeuf, V., S. Mounier, and J. Y. Benaim (2000), Solid phase extraction applied to natural waters: Efficiency and selectivity, *Org. Geochem.*, 31, 127–131.

Simoes, J. C., and V. S. Zagorodnov (2001), The record of anthropogenic pollution in snow and ice in Svalbard, Norway, *Atmos. Environ.*, 35, 403–413.

Staffelbach, T., A. Neftel, B. Stauffer, and D. Jacob (1991), A record of the atmospheric methane sink from formaldehyde in polar ice cores, *Nature*, 349, 603–605.

Stenson, A. C., A. G. Marshall, and W. T. Cooper (2003), Exact masses and chemical formulas of individual Suwannee River fulvic acids from ultrahigh resolution electrospray ionization Fourier transform ion cyclotron resonance mass spectra, *Anal. Chem.*, 75, 1275–1284.

Sumner, A. L., and P. B. Shepson (1999), Snowpack production of formaldehyde and its effect on the Arctic troposphere, *Nature*, 398, 230–232.

Thornton, D. C., A. R. Bandy, B. W. Blomquist, J. D. Bradshaw, and D. R. Blake (1997), Vertical transport of sulfur dioxide and dimethyl sulfide in deep convection and its role in new particle formation, *J. Geophys. Res.*, 102, 28,501–28,509.

Whelpdale, D. M., P. W. Summers, and E. Sanhueza (1997), A global overview of atmospheric acid deposition fluxes, *Environ. Monit. Assess.*, 48, 217–247.

Xie, S., T. Yao, S. Kang, B. Xu, K. Duan, and L. G. Thompson (2000), Geochemical analyses of a Himalayan snowpit profile: Implications for atmospheric pollution and climate, *Org. Geochem.*, 31, 15–23.

Yang, H., J. Xu, W. S. Wu, C. H. Wan, and J. Z. Yu (2004), Chemical characterization of water-soluble organic aerosols at Jeju Island collected during ACE-Asia, *Environ. Chem.*, 1, 13–17.

————————

A. M. Grannas, Department of Chemistry, Villanova University, Villanova, PA 19085, USA. (amanda.grannas@villanova.edu)

P. G. Hatcher, Department of Chemistry and Biochemistry, Old Dominion University, Norfolk, VA 23529, USA. (phatcher@odu.edu)

W. C. Hockaday, Department of Chemistry, Ohio State University, Columbus, OH 43210, USA.

E. Mosley-Thompson and L. G. Thompson, Byrd Polar Research Center, Ohio State University, Columbus, OH 43210, USA.